13th Australasian Fluid Mechanics Conference
Monash University, Melbourne, Australia
13-18 December 1998

A Turbulent Mechanism for Pulsation-Induced Orifice Plate Flow Meter Error

Lorenz W. SIGURDSON and Dallas D. CHAPPLE
4-9 Mechanical Engineering Building
Department of Mechanical Engineering
University of Alberta, Edmonton, Alberta, T6G 2G8 CANADA

ABSTRACT

Flow visualization and turbulent large-scale vortex structure theory is used to develop a more complete understanding of the flow physics involved in pulsation-induced error of orifice plate flow-rate meters. A test rig was designed and built to include fully turbulent pipe flow, smoke wire flow visualization, independent pulsation level control, and computer control and data acquisition. An *over-prediction* error of as much as 40% occurs when the highest levels of velocity pulsation are present at the orifice plate. This happens when the non-dimensional frequency of pulsation corresponds to the jet or shedding instabilities previously found in other flows. Analysis of photographs suggests that the error is caused by a modification of the vortices just downstream of the orifice plate. This narrows the vena contracta, reduces the downstream pressure and therefore increases the measured pressure drop for the same flow rate. For a narrower frequency range the converse can also occur, resulting in a much smaller *under-prediction.*

INTRODUCTION

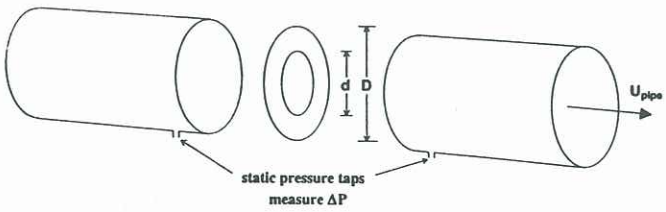

Figure 1 Exploded Schematic View of an Orifice Plate Flow Meter

The flow rate can be calculated from the measured pressure drop across the orifice (ΔP) using

$$Q = C_D \beta^2 \sqrt{\frac{2\Delta P}{\rho}} A_{pipe} = U_{pipe} A_{pipe},$$

where $Q$is the flow rate, C_D is the discharge coefficient, $\beta = \frac{d}{D}$ is the beta ratio, ρ is the fluid density, A_{pipe} is the pipe cross-sectional area, and U_{pipe} is the mean velocity in the pipe.

Although C_D is calibrated assuming a steady pipe flow, a large number of metering installations do not have steady flow. Pulsating flow can cause flow metering error and almost no previous research has included flow visualization or considered seriously the effect of large-scale vortex structures in turbulence. Our goal is to learn more about the fundamental physics of the problem using flow visualization.

Previous research has suggested various expected instability frequency regimes (Sigurdson and Chapple 1997) that are important to predicting the frequency response of the flow. They include the Kelvin-Helmholtz instability, the jet instability and the shedding instability of a separation bubble (Sigurdson 1995). This experiment indicates the relevance of this approach.

EXPERIMENTAL APPARATUS

A complex apparatus was designed and built that is capable of measuring the effect of pulsation on the C_D of an orifice plate flow meter. It used a computer to control the flow rate measurement, taking of photographs, and acquisition of: acoustic data, the pressure drop across the orifice plate, and other velocity and pressure data. It is the first instrument to combine these measurements with flow visualization. Control of the amplitude of pulsation was possible independent of flow rate. Two different beta ratios were tested.

Figure 2 shows an overall schematic diagram of the main test rig with most of the main aspects grouped into piping, Q section, test section, pulsation, air flow, and computer.

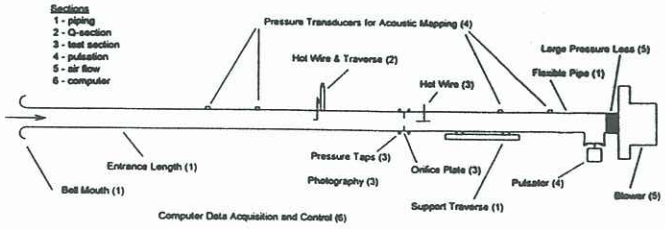

Figure 2 Main Rig Schematic View

The main experiments were conducted in a 146mm (nominal 6") diameter (ID) round pipe test rig. The operating point designed for was chosen to be 220 cm/s. Experiments were however also performed at velocities as low as approximately 90 cm/s and as high as 480 cm/s. This placed the shedding instability frequency at the center of the expected region of acoustic resonance of the pipe. The pipe had a total length of 13m once an extra section was added to accomodate measuring the acoustic pulsation levels.

The volume flow rate (Q) was measured using a hot-wire traverse at the Q section. The velocity profile was integrated numerically to give the flow rate. Control and measurement was done by a LabVIEW® program using a National Instruments DAQ board in a Pentium™ computer.

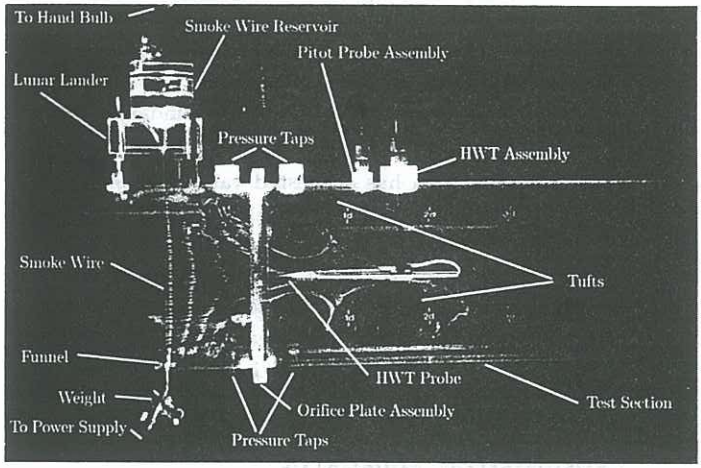

Figure 3 Test Section

Figure 3 shows the test section. The pressure taps and the hot-wire in the test section can also be seen here with the smoke wire upstream of the orifice plate. Photographs of the smoke were taken using a Nikon F2 35 mm camera with a 55 mm Micro Nikkor lens using Kodak TMax 3200 film developed at 3200 ASA.

The pulsation technique used a 1.59 mm thick acrylic plate attached flexibly to the base of a nominally 146 mm diameter "T" joint mounted on the pipe. The plate was forced using a B&K Vibration Exciter Type 4809, powered by an in-house built amplifier. The T was placed just upstream of the blower. Forcing was at pipe resonances to aid in producing higher pulsation levels and achieving a pure tone. The amplitude of the 1st harmonic was generally less than 3% of the fundamental frequency being forced.

To keep the pulsation level constant it was necessary to know the velocity magnitude at the orifice plate. Two pairs of pressure transducers up and downstream of the orifice were used to determine the acoustic pressure and velocity distribution in the pipe.

There was a correct concern that the pulsation would change the ΔP across the orifice and therefore the resulting volume flow rate in the test rig. To minimize this ΔQ we used a very large additional pressure loss immediately in front of the centrifugal blower. The blower was a turbo type of size 2T-10-28, SWSI, running at 3460 RPM with a 10 HP, 3 phase electric motor. It was found through experimentation that there was not a significant change in Q due to the effects of pulsation.

RESULTS AND DISCUSSION

Two important non-dimensional numbers are the Reynolds number (Re) and the Strouhal number (St). Re $=\frac{UD}{v}$ where U is the velocity, D is the pipe diameter and v is the kinematic viscosity. To nondimensionalize the pulsation frequency f_p two methods were used: the Strouhal number based on jet parameters $St_j = \frac{f_p d}{U_v}$ and shedding parameters $St_{sh} = \frac{f_p\left(\frac{D-d}{2}\right)}{U_v}$ (Sigurdson and Chapple 1997). The jet instability occurs near $St_j \approx 0.3$ and the shedding instability $St_{sh} \approx 0.8$ (although Sigurdson (1995) found a maximum flow response between values of 0.16 to 0.40).

The experimental conditions visited are given in Table 1. Pulsation velocity amplitudes (compared to the approximate velocity in the vena contracta U_v in %) ranged from 2 to 25% for the $\beta = 0.5$ plate. One experiment was done on the $\beta = 0.65$ plate at a level of 35%. The velocity was varied to check the Strouhal number scaling proposed, to give greater variation in pulsation amplitude, and to test the importance of Reynolds number. Several dozen rolls of film were exposed and over 1 gigabyte of measurement data was recorded.

Pulsation Level	Approx. U_{pipe}	Re
25%	1 m/s	9000
13%	1 m/s	9000
2%	5 m/s	47000
9%	2 m/s	20000
4.5%	2 m/s	20000
25%	1 m/s	9000
25%	1 m/s	9000
9%	1 m/s	9000
35%	1 m/s	9000

Table 1 Experimental Conditions

A Proposed Mechanism for Pulsation Induced Meter Error

We present here a proposed mechanism for pulsation induced meter error. It is primarily based on observations from photographs such as Figures 4, 5, 6. This is a mechanism for pulsation induced error due to influencing the large-scale vortex structures in the turbulence, whereas there are other ways pulsa-

tion can induce meter error. For example the high pressure amplitude but low Strouhal number pulsation discussed by Jungowski et al. (1990).

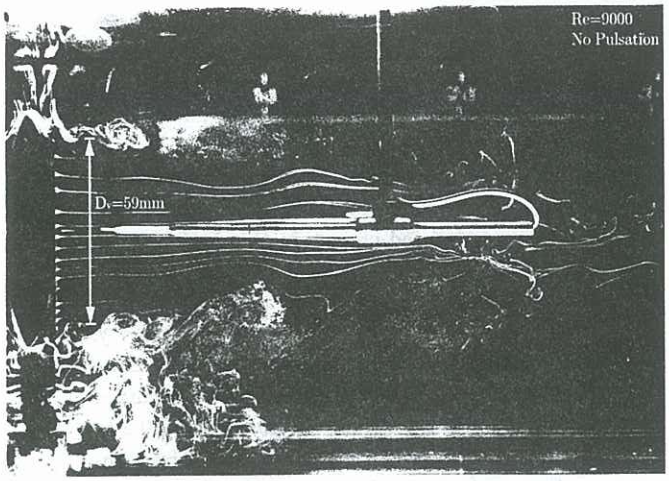

Figure 4 Streakline Photograph: No Pulsation $U_{pipe} = 0.96m/s, U_v = 5.9m/s, \Delta P = 24.4Pa$

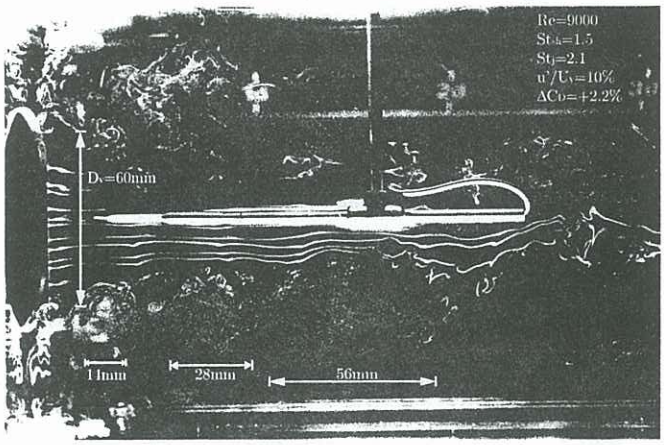

Figure 5 Streakline Photograph: $St_{sh} = 1.5, St_j = 2.1$, $U_{pipe} = 0.96m/s, U_v = 5.7m/s, \Delta P = 23.4Pa$

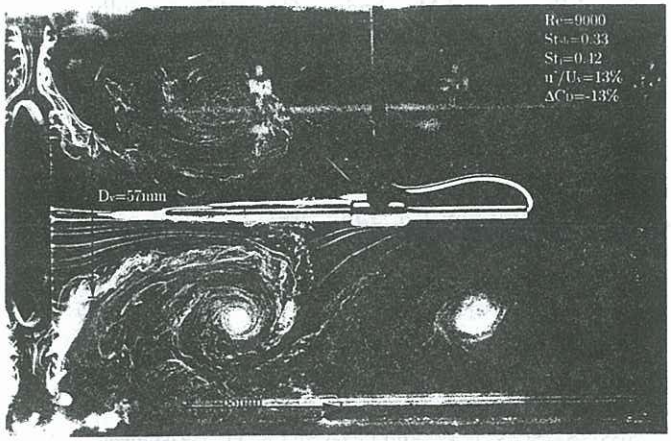

Figure 6 Streakline Photograph: $St_{sh} = 0.33, St_j = 0.42$, $U_{pipe} = 0.96m/s, U_v = 6.3m/s, \Delta P = 32.3Pa$

Here is the logical chain of concepts explaining meter error. In Figure 6 the vena contracta has been reduced due to the large vortex reaching into the core of the jet coming through the orifice plate, at least for the instant of the photograph. This reduction in vena contracta causes an increase in the velocity U_v, which by continuity is inversely proportional to the vena contracta diameter squared. A faster U_v translates to a reduction in the pressure downstream of the orifice plate via Bernoulli's equation. If it is assumed that the pressure upstream is unchanging, this is an explanation of why the pressure drop across the orifice plate is increasing. The flow rate is constant, therefore this leads to a negative error in the discharge coefficient (the actual discharge coefficient would be less than that predicted). The converse logic can be used to explain why a slight widening of the vena contracta would cause a positive error in the discharge coefficient. Following text will discuss details of these points.

Vortices are being shed at the edge of the orifice plate, convecting downstream, and pairing up as the shear layer grows. Figure 4 is with no pulsation, Figure 5 is with a high frequency of pulsation and Figure 6 is with a frequency of pulsation near where the largest effect occurred. Figure 5 shows the expected wavelength of 14 mm for a pulsation frequency of 198.5 Hz $\left(\lambda_\rho \approx \frac{U_v}{2f_p}\right)$. The frequency of pulsation for this photograph is above the shedding and jet instability range. Figure 6 shows a 68 mm vortex which corresponds to a pulsation frequency that is now in both the jet and shedding instability ranges. The vortex previously occurring further downstream in Figure 5 has moved right up to the orifice plate and the ΔC_D for this photograph is -13%. This is an example of the type of vortex modification which can cause a reduction of the vena contracta and meter error.

Even though we could not accurately ascertain the average vena contracta diameter $(D_v)$from the photographs, an indication of its relative size can be calculated using the measured Q and the hot-wire velocity in the test section. This value of D_v is shown in each Figure. Constant Q and a uniform velocity profile in the vena contracta were assumed (the former a good assumption, the latter less so), to give:

$$D_v = D\sqrt{\frac{U_{pipe}}{U_v}}.$$

An intriguing aspect of Figure 5 is that the estimated vena contracta is actually a little larger compared to the no pulsation case (2.5% more) and the pressure drop is a little smaller (4.2% less). The ΔC_D is + 2.5% which is smaller than our uncertainty (of 5%) in ΔC_D at this velocity, although the ΔC_D for the $\beta = 0.65$ run at $St_{sh} = 1.7$ is +8% which is greater than the uncertainty. This increase

in C_D happened in only a few of the cases tested, always at higher frequencies, and only the one had a ΔC_D greater than the uncertainty. It is likely that this higher frequency of pulsation is keeping the larger vortices farther away from the orifice plate where they have less of an effect. For a short portion of streamwise extent the pulsation slows down the growth of the shear layer by supressing pairing and therefore giving a wider vena contracta. This is known to happen in free shear layers (Oster and Wygnanski 1982).

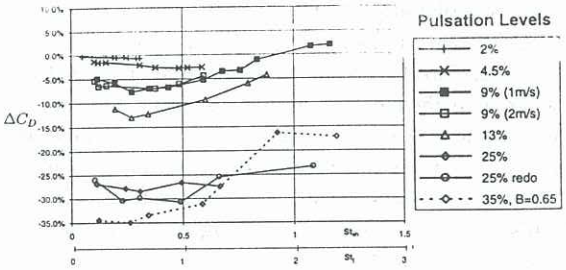

Figure 7 ΔC_D vs Non-dimensional Pulsation Frequency (St_jor St_{Sh}) at Different Pulsation Levels

The overall result of the pulsation on the flow is that, in most cases, the C_D is significantly reduced as shown in Figure 7. This graph gives the ΔC_D versus the non-dimensional frequency of pulsation, St_j and St_{sh}. As can be seen from this graph, there is significant effect in the same range of St for all levels of pulsation tested. The secondary x-axis of St_j is not valid for the 0.65 β run. For the 0.5 β ratio runs, St_j is double St_{sh}, since D_v is double H_v. This is only the case when the β ratio is 0.5 and so does not apply to the 0.65 β run. The St_{sh} is still valid.

The maximum effect is linear with pulsation level:
$\Delta C_{D\,\max}\% = 2\% - 1.15\left(\frac{u'}{U_v}\%\right)$.
Outside of this range of maximum effect, the amount of effect on the C_D drops off rapidly. Note the reproduceability in the repeat of the 25% pulsation run and in the 2 runs at 9% but at 2 different speeds. These are reasonably close to each other which demonstrates a repeatability in the tests, that the St scaling is correct, and that the Re is *not* important to the effect since it has doubled.

CONCLUSIONS

A mechanism for pulsation induced flow meter error has been proposed that is based on a change in behaviour of the flow due to a modification of the vortices. Pulsation within specific frequency regimes can result in larger vortices occurring closer to the orifice plate, a consequent narrowing of the vena contracta, and an increase in the pressure drop for the same flow rate. This causes a reduction in the effective discharge co-efficient from its calibrated value. Widening of the vena contracta can also occur with a converse result. Either way, it means meter error.

Three turbulent instabilities which have been identified in other flows, are present in orifice plate flow meters. These are the Kelvin-Helmholtz instability, jet instability, and shedding instability. Pulsation at the jet and shedding instability frequencies has been linked to a significant reduction in the discharge coefficient, while higher frequencies amplified by the Kelvin-Helmholtz instability have much less of an effect.

Significant metering error results to varying degrees depending on which instability is being forced. The maximum measured change in the discharge coefficient with pulsation was -30% for the 0.5 beta ratio orifice plate (-35% for the 0.65 beta ratio) at pulsation velocity amplitudes of 25% and 35% respectively. Put another way, the *indicated* flow rate would be 40% greater than the actual flow rate. This occurred for non-dimensional frequencies of pulsation of 0.2 to 0.5. The error occurred in a broad band of frequencies reaching to higher values, the range broadening as pulsation amplitude increased. This is very similar to the range found in forcing the separation bubble on a blunt-faced cylinder aligned coaxially with the free-stream (Sigurdson, 1995). Within this range, the maximum effect on the discharge coefficient was linear with pulsation velocity amplitude, and on initial inspection, apparently independent of pressure amplitude.

Forcing in a narrow range of non-dimensional frequencies about three times higher than those causing maximum meter error was seen to cause a small *increase* in discharge coefficient, 2.5% to 8% at very high amplitudes of forcing. This would *underpredict* the actual flow rate.

ACKNOWLEDGEMENTS

This work was funded primarily by NOVA Gas Transmission Limited and partly by National Sciences and Engineering Research Council of Canada Grant OGP 41747. The help of Mr. Blaine Sawchuk, Dr. Kamal Botros, and Mr. Andrew Coward is gratefully acknowledged.

REFERENCES

JUNGOWSKI, W., STUDZINSKI, W., and SZABO, J., "Orifice meter performance under pulsating flow conditions", *Internal Report for NOVA Natural Gas Transmission Co. Ltd.*, 1990.

OSTER, D. and WYGNANSKI, I., "The forced mixing layer between parallel streams", *J. of Fluid Mechanics*, **123**, 91-130, 1982.

SIGURDSON, L.W., "The structure and control of a turbulent reattaching flow", *J. of Fluid Mechanics*, **298**, 139-165, 1995.

SIGURDSON, L.W. and CHAPPLE, D., "Visualization of acoustically pulsated flow through an orifice plate flow meter", to appear, *J. Flow Visualization and Image Processing*, accepted 1997.